Since January 2020 Elsevier has created a COVID-19 resource centre with free information in English and Mandarin on the novel coronavirus COVID-19. The COVID-19 resource centre is hosted on Elsevier Connect, the company's public news and information website.

Advances in Medical Sciences 66 (2021) 403–410

Contents lists available at ScienceDirect

Advances in Medical Sciences

journal homepage: www.elsevier.com/locate/advms

Original research article

Association of echocardiographic parameters with chest computed tomography score in patients with COVID-19 disease

Faysal Saylik [a,*], Tayyar Akbulut [a], Mustafa Oguz [a], Abdulcabbar Sipal [a], Tolgahan Ormeci [b]

[a] Department of Cardiology, Van Education and Research Hospital, Van, Turkey
[b] Department of Radiology, Van Education and Research Hospital, Van, Turkey

ARTICLE INFO

Keywords:
BSTI score
Echocardiography
COVID-19
Mortality

ABSTRACT

Purpose: Although coronavirus disease 2019 (COVID-19) primarily affects the pulmonary system, the involvement of the heart has become a well-known issue. Pulmonary CT plays an additive role in the diagnosis and prognosis of the disease. We aimed to investigate the association of echocardiographic indices with pulmonary CT scores and mortality in COVID-19 patients.

Materials and methods: A total of 123 patients diagnosed with COVID-19 were included in this study. The British Society of Thoracic Imaging (BSTI) score and echocardiographic parameters were calculated, and echocardiographic indices were compared between BSTI score grades.

Results: During in-hospital follow-up, 36 of 123 patients (29.3%) had died. BSTI score, IVS, LVPWd, RV mid-diameter, RV basal diameter, RV longitudinal diameter, sPAP, and RVMPI were higher, and RVFAC, TAPSE, and RVS were lower in the non-survivor group than in the survivor group. There were statistically significant changes between BSTI scores in terms of LVPWd, RV mid diameter, RV basal diameter, RV longitudinal diameter, sPAP, RVFAC, RVMPI, and TAPSE. BSTI score was positively correlated with sPAP and RV basal diameter and negatively correlated with TAPSE and RVFAC. Multivariate logistic regression analysis demonstrated that sPAP (OR = 1.071, p = 0.002) and RV basal diameter (OR = 1.184, p = 0.005) were independent predictors of high BSTI scores (grade 4 and 5). Furthermore, age, sPAP, and a high BSTI score (grade 5) were independent predictors of in-hospital mortality in COVID-19 patients.

Conclusion: Echocardiographic indices were correlated with BSTI scores, and patients with higher BSTI scores had more cardiac involvement in COVID-19.

1. Introduction

Coronavirus disease 2019 (COVID-19), which is caused by a novel virus called severe acute respiratory syndrome coronavirus 2 (SARS-CoV-2), began spreading worldwide from Wuhan, Hubei, China, in December 2019. By August 06, 2021, over 201 million cases with a death rate of 2.1% had been reported from all countries [1]. COVID-19 primarily affects the lungs and contributes to pulmonary endothelial damage and parenchymal pneumonia, which finally causes acute respiratory distress syndrome. Although COVID-19 primarily affects the respiratory system, numerous other organs can be involved, leading to a pro-inflammatory cytokine storm with systemic inflammation and sepsis. The effect of COVID-19 on the cardiovascular system has been evaluated in previous studies, and complications such as myocardial damage, heart failure, venous thromboembolism, and arrhythmias have been reported to be more common in severe cases [2]. Angiotensin-converting enzyme 2 (ACE2) receptors, considered as the main entrance gate of SARS-CoV-2 into the cells, are present mainly in the epithelial cells of lungs but are also found in other organs such as the kidney and the heart [3]. Through the ACE2 receptor, viral entry into the artery vessels and myocardium can increase the risk of cardiac damage and inflammation [4]. It has been hypothesized that cardiac damage may be mediated by the interaction of SARS-CoV-2 with ACE2 or by the imbalance caused by altered functioning of the renin-angiotensin-aldosterone system [3]. Considering that aging is related to increasing deficiency of body functions, including the cardiovascular system, enhanced oxidative stress, and a diminished protective system [5], older adult patients are more vulnerable to aggressive adverse effects of viral infections such as COVID-19, including cardiac damage [3]. The tendency in older adult patients to have reduced viral clearance leads to cytokine storms with inappropriate immune

* Corresponding author. Department of Cardiology, Van Education and Research Hospital, Süphan Street, Airway Road, Van, 65100, Turkey.
E-mail address: faysalsaylik@gmail.com (F. Saylik).

https://doi.org/10.1016/j.advms.2021.08.001
Received 3 March 2021; Received in revised form 11 June 2021; Accepted 18 August 2021
Available online 21 August 2021

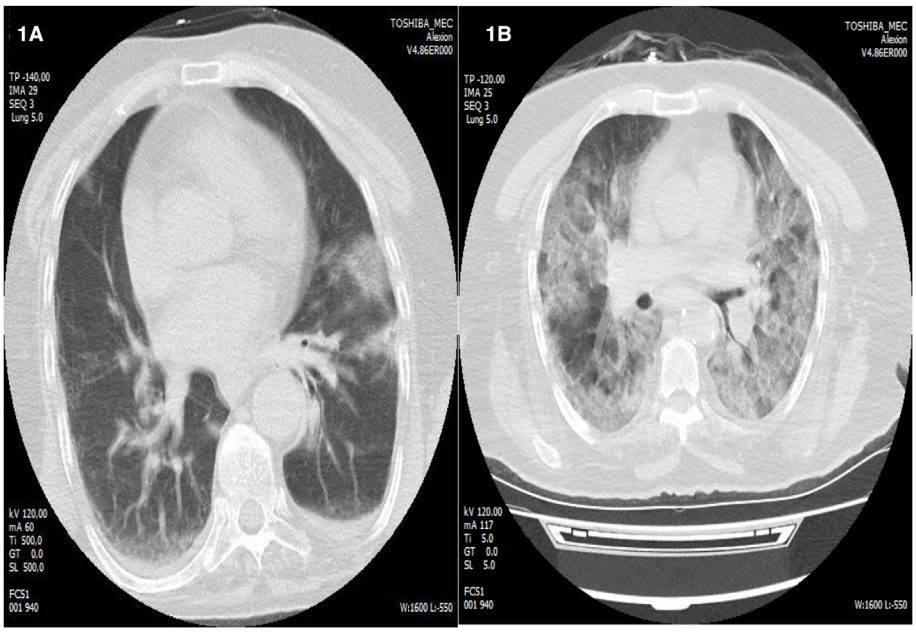

Fig. 1. Thoracic pulmonary computed tomography images from COVID-19 patients with BSTI score 2 who survived (1A) and with BSTI score 5 who did not survive (1B).

response. As a result, the infiltration of inflammatory cells, such as CD4 lymphocytes, macrophages, and neutrophils in the myocardium results in hyperemia, edema, cardiomyocyte hypertrophy, degeneration, and necrosis [3,5].

Due to its easy access and cost effectiveness, echocardiography is a useful tool used by cardiologists in their daily routine to investigate cardiac function. In a previous study, the significant effects of SARS-CoV-2 on the heart have been described as both left and right ventricular dilatation and depressed left and right ventricular functions [6]. Chest computed tomography (CT) is the first-choice imaging modality for detecting COVID-19 pneumonia. The most common COVID-19 characteristics that are visible in CT are ground-glass opacities (GGO), consolidations, interlobular septal thickening, crazy-paving pattern, air-bronchogram sign, reticular pattern, and mediastinal lymphadenopathies [7]. Several semi-quantitative scoring systems have been developed to assess the severity of pulmonary infection and to determine the correlation with disease severity. Pan et al. [8] described that the total score of pulmonary involvement increased progressively from the day of diagnosis to the 10th day after diagnosis. Wang et al. [9] reported similar CT score progression with a peak value on the 10th day after diagnosis. According to the severity of lung changes, the British Society of Thoracic Imaging (BSTI) ranked CT imaging into five grades from normal lungs to very severe disease, as described previously [10]. The present study aimed to investigate whether there is an association between echocardiographic parameters and the severity of pulmonary infiltration as graded by the BSTI.

2. Materials and methods

This retrospective study was conducted in 149 consecutive COVID-19 patients who were admitted to intensive care unit (ICU) of Van Education and Research Hospital, Van, Turkey, between April and October 2020. All patients underwent thoracic CT imaging upon admission to the emergency department for diagnosis of COVID-19 before transfer to the ICU. All echocardiographic evaluations were done with clinical indications based on cardiology consultation. In 26 patients, the chest CT image quality was too low for assessment, and their echocardiographic parameters were unmeasurable; hence, these patients were excluded from the study, and ultimately, the study included 123 patients. All participants had severe COVID-19 requiring non-invasive or invasive mechanical ventilation and follow-up in the ICU.

All patients were diagnosed with COVID-19 based on the reverse transcription-polymerase chain reaction (RT-PCR) on throat swab. Epidemiologic and demographic characteristics and routine hematologic and biochemical parameters (including troponin I, C-reactive protein (CRP), fibrinogen, and D-dimer) were collected and noted from hospital medical records. The laboratory analyses were performed using a Beckman Coulter LH 780 hematology analyzer (Beckman Coulter, FL, USA) for hematologic parameters and a Beckman Coulter LH 780 device (Beckman Coulter Ireland Inc., Mervue, Galway, Ireland) for biochemical parameters. Systemic immune-inflammation index (SIII) was calculated by neutrophil counts x platelet counts/lymphocyte counts [11].

2.1. Ethical issues

The study was approved by the ethics committee of Van Education and Research Hospital (approval No. 2021/02). This study, which involved human participants, was conducted in compliance with the 1964 Helsinki declaration and its later amendments.

2.2. Echocardiography

Due to the risk of viral transmission and the difficulty in achieving transthoracic echocardiography under rigorous isolation, echocardiography was performed in 123 consecutive COVID-19 patients on admission day to the ICU and recorded by one cardiologist. Then, the images were analyzed from the records by another cardiologist. All echocardiographic images were analyzed based on recent guidelines [12]. Apical and parasternal views were obtained using an $\times 5$ transducer (Philips Epiq7; Philips Healthcare, Inc., Andover, MA, USA). The echocardiographic parameters that were measured and noted included left ventricular ejection fraction (LVEF), interventricular septum diameter (IVSd) and left ventricular posterior wall diameter (LVPWd), right ventricular (RV) mid-diameter, RV basal diameter, RV longitudinal diameter, systolic pulmonary artery pressure (sPAP), RV myocardial performance index (RVMPI), tricuspid annular plane systolic excursion (TAPSE), RV fractional area change (RVFAC), and RV peak systolic tissue velocity at the tricuspid annulus (RVS). The RVMPI was calculated using formula (1)

$$RVMPI = \frac{isovolumetric\ contraction\ time + isovolumetric\ relaxation\ time}{ejection\ time}$$

as defined by Tei et al. [13]. TAPSE was measured by M-mode recordings of free wall of the tricuspid annulus from apical 4-chamber view, as previously recommended [14]. RVFAC was calculated using formula (2)

$$RVFAC = \frac{RV\ end - diastolic\ area - RV\ end - systolic\ area}{RV\ end - diastolic\ area}\ x100$$

[15]. RVS was gained by placing the sample volume on the tricuspid annulus, as previously described [16]. All pulsed wave Doppler imaging parameters were calculated as the mean value of 5–8 consecutive heart cycles.

2.3. Computed tomography

All chest CT images were taken using the Alexion 16 Slice CT scanner (Toshiba Medical Systems, Nasu, JAPAN). After topogram images were taken, the scanning area was determined appropriately by calculating details such as diaphragm height, upper limit of thorax, and breathing space. Then, the chest CT images were taken axially for the thoracic region with settings of 120 kVp, 50 mAs, range 500, 5 mm slice thickness, and 90–110 mean number of sections. The received raw data were organized in multiplanar reformation (MPR) formatting. All images were examined by two radiology experts. In case of disagreement, the final decision of a third radiologist, who had 10 years of experience and was aware of the study, was accepted.

In this study, patients were evaluated anatomically based on the severity of the involvement of lung lobes. In the evaluation phase, areas of ground-glass density, consolidation, nodular opacities, presence of air bronchograms, inverted halo findings, air bubble findings, presence of vascular enlargement, pleural thickening, pleural effusion, and pleural retraction were reviewed. To evaluate the segmental and lobar distribution and severity of the COVID-19, the findings were considered and graded according to the BSTI COVID-19 severity scoring system, i.e. 1-normal lung, 2-mild (<25%), 3-moderate (26–50%), 4-heavy (51–75%), 5-very heavy (>75%) (Fig. 1) [10]. The lung changes that were not associated with COVID-19 were classified as 1-normal lung.

2.4. Statistical analysis

Statistical analyses were conducted using SPSS software (version 22.0, SPSS Inc., Chicago, IL, USA). The Kolmogorov-Smirnov test was used to determine the normality of the data. Quantitative variables with a normal distribution were represented as the arithmetical mean ± standard deviation, whereas those without normal distribution were designated as the median (25th – 75th interquartile range). Categorical variables were denoted as numbers and percentages. The unpaired student's *t*-test was used to compare normally distributed variables. The Mann-Whitney *U* test was used for non-normal distribution between the survivor and non-survivor groups. The chi-squared test and Fisher's exact test with Freeman and Hamilton's correction were used to compare categorical variables, when appropriate. For comparing variables between CT score grades, one-way ANOVA or the Kruskal-Wallis test was used. In post-hoc analysis, Tukey's or Dunn's procedure with a Bonferroni adjustment was used, where appropriate. Spearman correlation analysis was performed to detect the correlation between the CT scores and the echocardiographic and laboratory parameters. Prediction of high BSTI scores (grades 4 and 5) with echocardiographic indices was calculated using logistic regression analysis. For detecting independent predictors of in-hospital mortality due to COVID-19, univariate logistic regression analysis was used. Because of the small event size of outcome (number of deaths = 36), only four clinically relevant variables that exhibited significant association in univariate logistic regression analysis were included in multivariate logistic regression analysis. A weighted-kappa statistic for CT scores was used to check interobserver reliability, and a kappa value of 0.968 of CT scores (p-value <0.0001) was obtained with excellent agreement between radiologists. A p-value of less than 0.05 was considered statistically significant.

Table 1
Demographic, clinical, laboratory, echocardiogarphic and CT findings of patients in survivor and non-survivor groups of COVID-19.

Variables	Non-survivor group (N = 36)	Survivor group (N = 87)	p value
Age, years	70.2 ± 9.8	62 ± 12.9	0.001
Gender, male, n (%)	22 (61.1)	42(48.3)	0.195
DM, n (%)	12(33.3)	17(19.5)	0.101
HT, n (%)	16(44.4)	31(35.6)	0.36
Cigarette smoking, n (%)	4(11.1)	8(9.2)	0.745
COPD, n (%)	5(13.9)	10(11.5)	0.765
CAD, n (%)	4(11.1)	10(11.5)	0.999
CVD, n (%)	3(8.3)	4(4.6)	0.416
Malignancy, n (%)	1(2.8)	1(1.1)	0.501
WBC, cells/μL	13.5(9.8–17.8)	9.8(8–13.8)	0.008
Hemoglobin, g/dL	12.9 ± 2.4	13.4 ± 1.9	0.253
Platelet, cells/μL	222.3 ± 116.3	235.8 ± 78.7	0.455
Neutrophil, cells/μL	10.7(8.5–13.2)	8.2(6.6–10.6)	0.007
Lymphocyte, cells/μL	0.55(0.35–0.93)	0.81(0.64–1)	0.004
Monocyte, cells/μL	0.35(0.19–0.65)	0.45(0.33–0.65)	0.096
MPV, %	11.2 ± 1.6	10 ± 1.6	0.001
RDW, %	50.5(45.8–60.2)	45.1(41.4–50.9)	<0.001
SIII	3346(1730–5588)	1780(988–3689)	0.004
Sodium, mEq/L	141.5(136.2–147.5)	141(138–145)	0.715
BUN, mg/dL	68.7(49.7–107.2)	58(36–88)	0.075
Creatinine, mg/dL	0.9(0.6–1.3)	0.9(0.8–1.1)	0.640
Potassium, mEq/L	4.4 ± 0.6	4.3 ± 0.6	0.759
Magnesium, mEq/L	2.2 ± 0.4	2.1 ± 0.3	0.011
Calcium, mEq/L	8.2 ± 0.6	8.6 ± 0.5	<0.001
Ferritin, ml/ng	1229(771–1698)	448(196–1075)	<0.001
Albumin, g/L	3.05 ± 0.59	3.5 ± 0.58	<0.001
CRP, mg/dL	104.5(58.8–143.8)	18.5(8.6–69.1)	<0.001
D-dimer, μg/mL	1758(635–5020)	362(179–1627)	<0.001
Fibrinogen, mg/L	343.4 ± 100.9	316.7 ± 90.8	0.154
Troponin I, ng/mL	0.29(0.1–1.3)	0.1(0.1–0.21)	<0.001
BSTI score	4.5(3–5)	2(2–4)	<0.001
Echocardiographic measurements			
Ejection fraction, %	60(60–65)	64(60–65)	0.051
IVSd, mm	12(11–13)	11(10–13)	0.034
LVPWd, mm	12(11–13)	11(10–12)	0.003
RV mid diameter, mm	37(34–46)	34(32–37)	0.002
RV basal diameter, mm	42(38–45)	39(38–42)	0.026
RV longitudinal diameter, mm	73 ± 6.7	65.7 ± 7.6	<0.001
sPAP, mmHg	45.3 ± 13.1	32.2 ± 11.5	<0.001
RVFAC, %	38(34.2–40)	42(38–44)	<0.001
RVMPI	0.64 ± 0.14	0.54 ± 0.13	<0.001
TAPSE, mm	16.5 ± 4.4	20.7 ± 5.7	<0.001
RVS, cm/s	15.2 ± 3.1	16.5 ± 2.9	0.035

Abbreviations: DM, Diabetes mellitus; HT, Hypertension; COPD, Chronic obstructive pulmonary disease; CAD, Coronary artery disease; CVD, Cerebrovascular disease; WBC, White blood cells; MPV, Mean platelet volume; RDW, Red cell distribution width; SIII, Systemic immune-inflammation index; BUN, blood urea nitrogen; CRP, C-reactive protein; BSTI, British Society of Thoracic Imaging; RV, Right ventricle; sPAP, Systolic pulmonary arterial pressure; RVFAC, right ventricular fractional area change; RVMPI, right ventricular myocardial performance index; TAPSE, tricuspid annular plane systolic excursion; RVS, right ventricular peak systolic tissue velocity at the tricuspid annulus; IVSd, Interventricular septum; LVPWd, Left ventricular posterior wall diameter.

3. Results

In the present study, we included 123 consecutive patients diagnosed with COVID-19. During in-hospital follow-up, 29.3% (n = 36) of patients died. The mean age in the non-survivor group was 70.2 ± 9.8 and 61.1% were male, whereas in the survivor group, the mean age was 62 ± 12.9, and 48.3% were male. The non-survivor group was older than the

Table 2
Comparison of demographic, laboratory, and echocardiographic parameters based on CT grades according to British Society of Thoracic Imaging.

Variables	Grade 1 (n = 13)	Grade 2 (n = 46)	Grade 3 (n = 13)	Grade 4 (n = 20)	Grade 5 (n = 31)	p value
Age, years	63(52.5–65.5)	66(54–75)	67(56.5–79.5)	64.5 (57.270.7)	69(59–74)	0.246
Gender, male, n (%)	7(53.8)	22(47.8)	5(38.5)	13(65)	17(54.8)	0.601
DM, n (%)	1(7.7)	13(28.3)	3(23.1)	5(25)	7(22.6)	0.688
HT, n (%)	3(23.1)	22(47.8)	1(7.7)	8(40)	13(41.9)	0.067
COPD, n (%)	1(7.7)	6(13)	1(7.7)	2(10)	5(16.1)	0.968
CAD, n (%)	1(7.7)	8(17.4)	0(0)	2(10)	3(9.7)	0.580
CVD, n (%)	0(0)	2(4.3)	2(15.4)	0(0)	3(9.7)	0.260
Malignancy n (%)	0(0)	1(2.2)	0(0)	0(0)	1(3.2)	0.999
WBC, cells/μL	9.1(8–10.4)	10.1(7.9–14)	12.5(6.8–14.6)	12.9(8.8–16.3)	13.8(9.6–17.3)	0.019
Lymphocyte, cells/μL	0.67(0.61–0.75)	0.83(0.47–1.29)	0.90(0.35–2)	0.68(0.42–0.8)	0.78(0.62–0.99)	0.451
Albumin, g/L	4.1(3.9–4.2)	3.6(3–4)	3.4(2.9–3.8)	3.2(2.8–3.6)	3.1(2.8–3.6)	<0.001
Ferritine, ml/ng	227(198–250)	345(176–934)	512(214–1070)	882 (516–1656)	1320 (849–1700)	<0.001
Fibrinogen, mg/L	202(180–234)	341(298–366)	358(318–399)	354(242–416)	342(311–438)	<0.001
D-dimer, μg/mL	302(233–359)	314(151–1231)	488(190–1168)	2228(857–3329)	2156(685–6589)	<0.001
CRP, mg/dL	7.9(3.9–12.8)	26.3(9.9–64.4)	47(14.3–146.5)	73.8(39–174.5)	97.1(17–144)	<0.001
Troponin I, ng/mL	0.1	0.1(0.1–0.12)	0.1(0.1–0.29)	0.35(0.1–0.64)	0.46(0.1–1.4)	<0.001
Death, n (%)	0(0)	8(17.4)	5(38.5)	5(25)	18(58.1)	<0.001
Echocardiographic indices						
Ejection fraction, %	65(60–66)	64(60–65)	64(60–65)	61(58.5–64.5)	62(60–65)	0.170
IVSd, mm	12(11–12)	10.5(10–13)	12(10–13)	12(10.2–13.7)	12(11–14)	0.06
LVPWd, mm	11(10–11.5)	10(9–11.5)	12(9.5–13)	11.5(10–13)	12(11–13)	0.011
RV mid diameter, mm	33(30–34)	34.5(32–37.2)	35(33–37)	35(30.5–40.7)	38(33–47)	0.016
RV basal diameter, mm	37(35–39)	39(37.7–42)	38(36.5–39)	40(38–42)	44(39–49)	<0.001
RV longitudinal diameter, mm	66(62.5–69)	64.5(60–69.2)	65(60–73)	68.5(65–76.5)	70(65–78)	0.014
sPAP, mmHg	27(23–29.5)	27(18.7–40)	33(28.5–47)	42.5(35–54.5)	43(32–49)	<0.001
RVFAC, %	44(41.5–45.5)	42(37.7–45)	40(36–41.5)	39(37–40)	38(34–41)	<0.001
RVMPI	0.48(0.47–0.53)	0.54(0.45–0.60)	0.50(0.40–0.55)	0.52(0.49–0.67)	0.63(0.51–0.73)	0.03
TAPSE, mm	26(20–28)	19.5(16–25)	19(17.5–25)	18.5(14.2–23)	15(13–20)	<0.001
RVS, cm/s	14(12–17)	17(14.7–19)	16(14–17)	16(14.2–18)	17(15–18)	0.062

Abbreviations: DM, Diabetes mellitus; HT, Hypertension; COPD, Chronic obstructive pulmonary disease; CAD, Coronary artery disease; CVD, Cerebrovascular disease; WBC, White blood cell; CRP, C-reactive protein; IVSd, Interventricular septum diameter; LVPWd, Left ventricular posterior wall diameter; RV, Right ventricle; sPAP, Systolic pulmonary arterial pressure; RVFAC, right ventricular fractional area change; RVMPI, right ventricular myocardial performance index; TAPSE, tricuspid annular plane systolic excursion; RVS, right ventricular peak systolic tissue velocity at the tricuspid annulus.

survivor group (p = 0.001). There were no statistically significant differences between the survivor and non-survivor groups in terms of comorbidities. The non-survivor group had higher white blood cell count (WBC), neutrophil, mean platelet volume (MPV), red cell distribution width (RDW), SIII, ferritin, C-reactive protein (CRP), D-dimer, and troponin I levels, and lower lymphocyte counts when compared to the survivor group. BSTI score was higher in non-survivors than survivors (p < 0.001). In terms of echocardiographic parameters, IVSd, LVPWd, RV-mid diameter, RV basal diameter, RV longitudinal diameter, sPAP, and RVMPI were higher, and RVFAC, TAPSE, and RVS were lower in the non-survivor group versus the survivor group. Other demographic, clinical, and laboratory features of patients are presented in Table 1.

In Table 2, we demonstrate the comparison of parameters between five chest CT grades stratified according to BSTI. There were no statistically significant differences between the groups with regard to age, sex, and comorbidities. There were statistically significant differences between the chest CT grades in terms of WBC, albumin, ferritin, fibrinogen, D-dimer, CRP, troponin I, death rate, LVPWd, RV-mid diameter, RV basal diameter, RV longitudinal diameter, sPAP, RVFAC, RVMPI, and TAPSE. In post hoc analyses, patients with chest CT grade 5 had higher fibrinogen, D-dimer, troponin I, RV-mid diameter, sPAP, RVMPI, and lower RVFAC and TAPSE than those with grade 1. D-dimer, troponin I, and sPAP were higher, and RVFAC and TAPSE were lower in patients with chest CT grade 5 than in those with grade 2. Grade 5 patients had a higher D-dimer and RVMPI than those with grade 3. Grade 4 patients had higher fibrinogen, D-dimer, troponin I, and sPAP, and lower RVFAC than those with grade 1. sPAP and D-dimer levels were higher in patients with chest CT grade 4 than in patients with grade 2. Grade 3 patients had higher fibrinogen and troponin I than patients with grade 1. Grade 2 patients had higher troponin I and fibrinogen than patients with grade 1. Finally, the death rates were higher among patients with grades 3, 4, and 5 than those with grades 1 or 2. Other comparisons are summarized in detail in Table 2.

Table 3
Correlations of BSTI score with echocardiography indices and laboratory parameters.

Variables	Correlation coefficient	p value
Troponin I	0.572	<0.001
D-dimer	0.525	<0.001
Fibrinogen	0.371	<0.001
Ferritine	0.511	<0.001
CRP	0.436	<0.001
Albumin	−0.447	<0.001
sPAP	0.464	<0.001
TAPSE	−0.377	<0.001
LVPWd	0.287	0.001
RV basal diameter	0.423	<0.001
RV longitudinal diameter	0.286	0.001
RVFAC	−0.400	<0.001
RVMPI	0.311	<0.001

Abbreviations: BSTI, British Society of Thoracic Imaging; CRP, C-reactive protein; sPAP, Systolic pulmonary arterial pressure; TAPSE, tricuspid annular plane systolic excursion; LVPWd, Left ventricle posterior wall diameter; RV, Right ventricle; RVFAC, right ventricular fractional area change; RVMPI, right ventricular myocardial performance index.

BSTI score was positively correlated with troponin I, D-dimer, ferritin, sPAP, RV basal diameter and negatively correlated with TAPSE and RVFAC (Table 3) (Fig. 2). Multivariate logistic regression analysis demonstrated that sPAP [OR = 0.071(1.026–1.119), p = 0.002] and RV basal diameter [OR = 1.184(1.053–1.332), p = 0.005] were independent predictors of high BSTI score (grade 4 and 5) (Table 4). A cut-off value of sPAP for detecting high BSTI scores (grade 4 and 5) was 30.5 with a sensitivity of 90.2% and specificity of 61.1% in receiver-operating characteristic (ROC) curve analysis (Fig. 3). In Table 5, we show that age, sPAP, and a higher BSTI score (grade 5) were independent predictors of in-hospital mortality of COVID-19 patients.

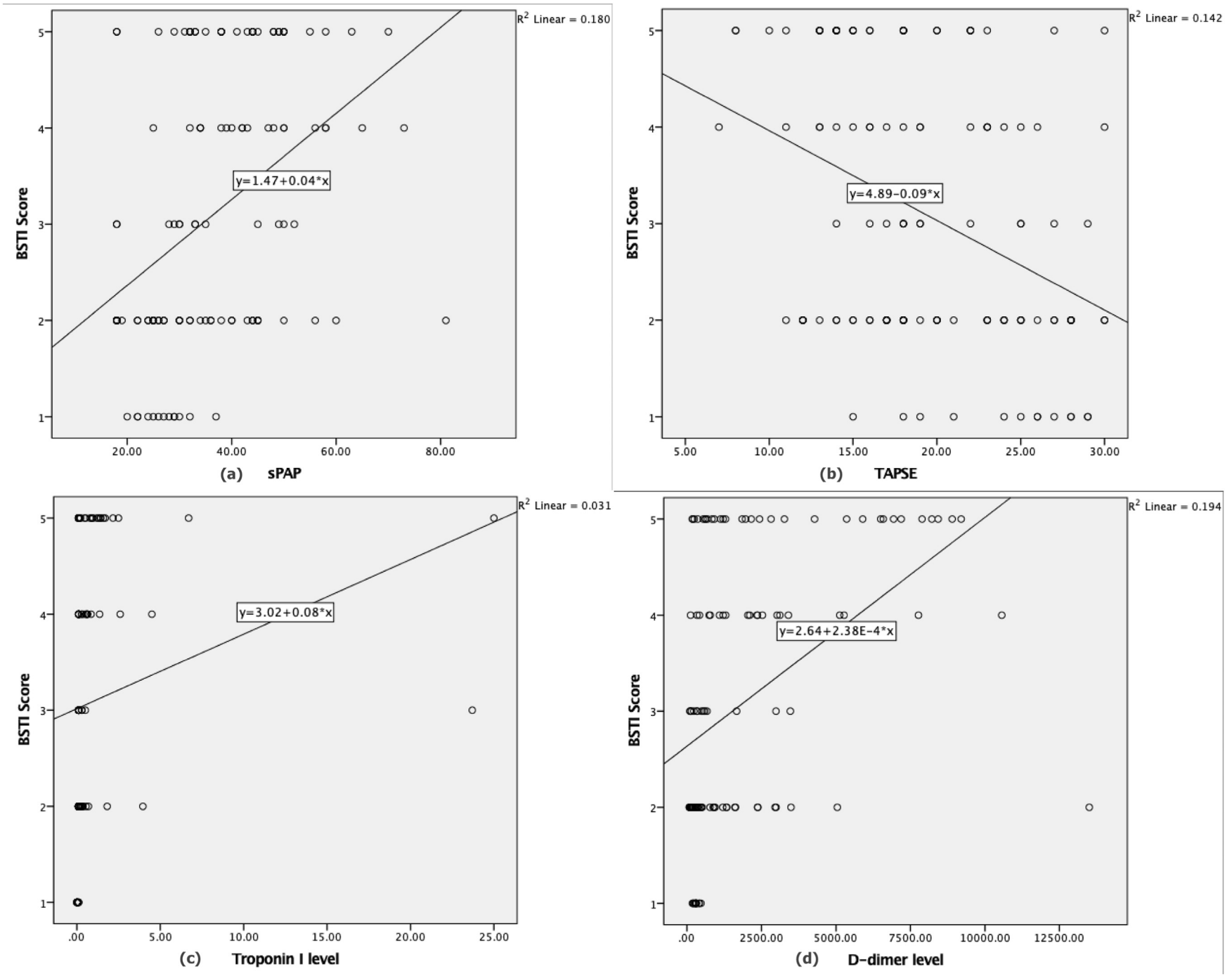

Fig. 2. Correlation plots of a) sPAP, b) TAPSE, c) Troponin-I levels, d) D-dimer with BSTI scores.

Table 4
Univariate and multivariate logistic regression analysis of echocardiographic parameters for detecting independent predictors of high (grade 4 and 5) BSTI score of chest CT.

Variables	Univariate OR, 95%CI	p value	Multivariate OR, 95CI	p value
TAPSE	0.880(0.819–0.946)	0.001	0.946(0.859–1.040)	0.251
sPAP	1.083(1.045–1.122)	<0.001	1.071(1.026–1.119)	0.002
RV longitudinal diameter	1.083(1.031–1.138)	0.002	0.980(0.914–1.052)	0.580
RV basal diameter	1.229(1.109–1.362)	<0.001	1.184(1.053–1.332)	0.005
RVFAC	0.874(0.806–0.949)	0.001	1.035(0.920–1.164)	0.571
RVMPI	141.920(7.569–2661.161)	0.001	1.122(0.015–83.062)	0.958

Abbreviations: TAPSE, tricuspid annular plane systolic excursion; sPAP, Systolic pulmonary arterial pressure; RV, Right ventricle; RVFAC, right ventricular fractional area change; RVMPI, right ventricular myocardial performance index; BSTI, British Society of Thoracic Imaging; CT, computed tomography.

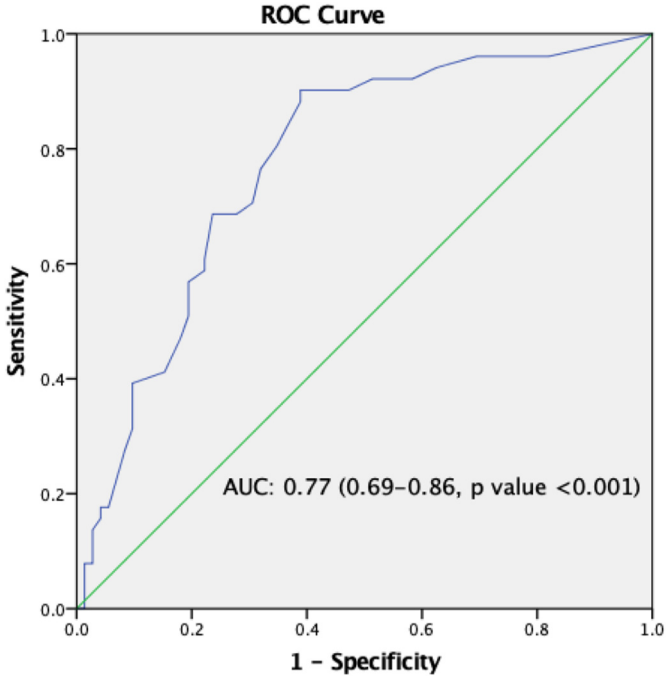

Fig. 3. ROC analysis of sPAP for detecting high BSTI scores (grade 4 and 5).

4. Discussion

This study showed that echocardiographic indices were correlated with BSTI scores and that patients with higher BSTI scores had more cardiac involvement in the course of COVID-19. sPAP and RV basal diameter were independent predictors of high BSTI scores (grades 4 and 5).

COVID-19 infection has broad clinical spectrum, varying from asymptomatic to severe progressive pneumonia that can lead to multi-organ failure and death [17]. The cardiovascular complications of COVID-19 have been reported as myocardial injury, arrhythmias, myocarditis, and venous thromboembolism [18]. Xu et al. [6] reported that age, increased CRP levels, and comorbidities were independent risk factors for cardiac involvement. It is known that cardiac involvement and dysfunction are associated with a worse prognosis in COVID-19 patients [19]. The pathogenesis of cardiac involvement of COVID-19 might possibly be due to damage to the heart directly by the virus and the degeneration and necrosis of cells with hyaline thrombus formation in small vessels [20]. Although SARS-CoV-2 viral particles were not isolated in the myocardium, they were detected in interstitial macrophages with myofibrillar lysis [21]. The indirect effects of the virus could be seen in the myocardium as morphological changes, including lymphomonocytic infiltration, interstitial edema, and myocytolysis [22]. Endothelial cells of the heart and several organs are infected by the virus directly via a main entrance receptor, ACE2, which causes diffuse inflammation [23]. Inflammation and hypoxia in the lungs lead to alveolar and pulmonary capillary damage with an increase in pulmonary vascular resistance,

Table 5
Univariate and multivariate logistic regression analysis for detecting in-hospital death due to COVID-19 disease.

Variables	Univariate OR, (95%CI)	p value	Multivariate OR, (95%CI)	p value
Age	1.066(1.024–1.109)	0.002	1.061(1.010–1.115)	0.019
Lymphocyte	0.295(0.107–0.814)	0.018	–	–
Ferritine	1.001(1.000–1.001)	0.006	–	–
Albumin	0.227(0.107–0.479)	<0.001	–	–
CRP	1.007(1.002–1.013)	0.007	–	–
D-dimer	1.000(1.000–1.000)	0.008	–	–
Troponin I	1.644(1.018–2.655)	0.042	–	–
BSTI score[a]				
Score 3 and 4	2.772(0.968–7.936)	0.058	1.544(0.460–5.184)	0.482
Score 5	8.827(3.146–24.767)	<0.001	5.383(1.621–17.870)	0.006
IVSd	1.104(0.938–1.298)	0.234	–	–
LVPWd	1.187(0.974–1.447)	0.089	–	–
RV mid diameter	1.104(1.040–1.171)	0.001	–	–
RV basal diameter	1.117(1.030–1.211)	0.008	–	–
RV longitudinal diameter	1.135(1.071–1.203)	<0.001	–	–
sPAP	1.088(1.048–1.130)	<0.001	1.069(1.026–1.114)	0.001
RVFAC	0.837(0.764–0.917)	<0.001	–	–
RVMPI	208.3(10.003–4339.599)	0.002	–	–
TAPSE	0.861(0.792–0.935)	<0.001	0.949(0.862–1.044)	0.280
RVS	0.871(0.763–0.993)	0.039	–	–

Abbreviations: CRP, C-reactive protein; BSTI, British Society of Thoracic Imaging; IVSd, Interventricular septum diameter; LVPWd, Left ventricular posterior wall diameter; RV, Right ventricle; sPAP, Systolic pulmonary arterial pressure; RVFAC, right ventricular fractional area change; RVMPI, right ventricular myocardial performance index; TAPSE, tricuspid annular plane systolic excursion; RVS, right ventricular peak systolic tissue velocity at the tricuspid annulus.

[a] Reference category is BSTI score 1 and 2.

representing an increase in RV afterload [24]. The most common findings among critically ill COVID-19 patients were RV dilatation and dysfunction [17]. Many conditions contribute to RV dysfunction in COVID-19 patients, including pulmonary embolism, hypoxic pulmonary vasoconstriction, pneumonia, elevated positive end-expiratory pressure, hypercarbia, decreased lung volume, and elevated left atrial pressure or a combination of all these [17]. The severity of RV dysfunction was established as an independent predictor of mortality in various patients. Li et al. [25] showed RV dilatation and dysfunction in non-survivor COVID-19 patients and reported that a global right ventricular longitudinal strain (RVLS) $<$ 23% might be an independent predictor of in-hospital death. Other echocardiographic abnormalities of COVID-19 have been reported in previous studies as LV and RV enlargement, both LV and RV systolic and diastolic dysfunction, pulmonary hypertension, pericardial effusion, and abnormal strain patterns [26,27]. The correlation and additive value of echocardiography to lung ultrasound has been reported by Szekely et al. [28]. The authors reported that a very limited echocardiographic examination might be sufficient to generate a strategy for risk stratification in COVID-19 patients.

Due to the false-negative results of RT-PCR, chest CT has become an important diagnostic imaging modality, especially in patients with negative test results but with a high clinical probability of COVID-19 [7]. The infiltration of SARS-CoV-2 into pneumocytes generates an inflammatory cytokine storm, which leads to acute interstitial lung damage and pneumonia [29–31]. The most frequent chest CT findings of patients with COVID-19 are GGO and consolidation, which are the results of hyaline membrane formation, alveolar exudates, and pulmonary edema [31–33]. The distribution of parenchymal infiltrates of the lungs was frequently bilateral (87.5%), multilobar, (78.8%), and peripheral (76%), with especially posterior regions' involvement (80.4) [34]. Several semi-quantitative CT scores have been calculated to assess the severity of pulmonary infiltration [35,36]. Yang et al. [35] developed a CT scoring system that calculates the percentage of opaque involvement of 20 segments of the lungs, in which scores were defined as 0% as zero points, 1–50% as 1 point, >50% as 2 points, with a maximum of 40 points in total. The cut-off value was 19.5 points to estimate the severe cases in this study. Yuan et al. [37] calculated a CT score based on the location, distribution, and extent of the pulmonary findings, which ranged from 0 to 72. They found that non-survivors had a higher CT score than survivors, and a cut-off value of 24.5 was noted for predicting mortality. The BSTI score ranks the pulmonary changes into five grades i.e., normal lungs - 1, mild (≤25%) - 2, moderate (26–50%) - 3, severe (51–75%) - 4, and very severe (≥75%) - 5. The association between echocardiography parameters and the severity of COVID-19 has been established in previous studies based on clinical findings. Patients with severe COVID-19 had lower LVEF, higher dimensions of left and right ventricles, higher rates of left ventricular diastolic dysfunction, and higher left ventricular global longitudinal strain, as well as higher sPAP than non-severe patients, especially in participants with mechanical ventilation [27,38]. However, there is no information in the literature about the relationship between echocardiographic indices and grades of chest pulmonary CT score.

4.1. *Limitations of the study*

The retrospective study design and small sample size are the major limitations of this study. Another limitation is the absence of echocardiographic parameters for all patients before and after the COVID-19 infection. Because all patients included in this study had severe illness and were admitted to the ICU, results cannot be generalized to patients with no symptoms or with mild disease. Echocardiography was performed based on the clinical indication, which might contribute to overestimation of abnormal echocardiographic findings in those patients. Further prospective studies with a large sample size should be carried out to establish the association between echocardiographic indices and pulmonary CT grades.

5. Conclusions

The main findings of this study were that BSTI scores were correlated with echocardiographic indices, i.e. patients with high BSTI scores had altered echocardiographic parameters when compared to patients with low BSTI scores, and echocardiographic parameters such as sPAP and RV basal diameter were independent predictors of high BSTI scores. Furthermore, non-survivor COVID-19 patients had higher BSTI scores and altered echocardiographic parameters when compared to surviving patients. Both BSTI scores and echocardiographic parameters were independent predictors of mortality in those patients. Because of its easy access and low cost, echocardiography might be used for risk stratification in COVID-19 patients with correlated pulmonary CT infiltration.

Financial disclosure

The authors have no funding to disclose.

The author contributions

Study design: Faysal Saylik.
Data collection: Tayyar Akbulut, Mustafa Oguz.
Statistical Analysis: Faysal Saylik.
Data interpretation: Faysal Saylik.
Manuscript preparation: Faysal Saylik, Tayyar Akbulut, Tolgahan Ormeci.
Literature search: Faysal Saylik, Mustafa Oguz, Abdulcabbar Sipal.
Funds Collection: n/a.

Declaration of competing interest

The authors declare no conflict of interests.

References

[1] The Johns Hopkins Coronavirus Resource Center (CRC). [Available from: https://coronavirus.jhu.edu/map.html.
[2] Shafi AM, Shaikh SA, Shirke MM, Iddawela S, Harky A. Cardiac manifestations in COVID-19 patients—a systematic review. J Card Surg 2020 Jul;35(8):1988–2008. https://doi.org/10.1111/jocs.14808.
[3] Mansueto G, Niola M, Napoli C. Can COVID 2019 induce a specific cardiovascular damage or it exacerbates pre-existing cardiovascular diseases? Pathol Res Pract 2020 Sep;216(9):153086. https://doi.org/10.1016/j.prp.2020.153086.
[4] Napoli C, Tritto I, Benincasa G, Mansueto G, Ambrosio G. Cardiovascular involvement during COVID-19 and clinical implications in elderly patients. A review. Ann. Med. Surg. 2020 Sep;57:236–43. https://doi.org/10.1016/j.amsu.2020.07.054.
[5] Napoli C, Tritto I, Mansueto G, Coscioni E, Ambrosio G. Immunosenescence exacerbates the COVID-19. Arch Gerontol Geriatr 2020 Sep-Oct;90. https://doi.org/10.1016/j.archger.2020.104174. 104174-104174.
[6] Xu H, Hou K, Xu R, Li Z, Fu H, Wen L, et al. Clinical characteristics and risk factors of cardiac involvement in COVID-19. J. Am. Heart Assoc. 2020 Aug;9(18):e016807. https://doi.org/10.1161/JAHA.120.016807.
[7] Cellina M, Orsi M, Pittino CV, Toluian T, Oliva G. Chest computed tomography findings of COVID-19 pneumonia: pictorial essay with literature review. Jpn J Radiol 2020 Jun;38(11):1012–9. https://doi.org/10.1007/s11604-020-01010-7.
[8] Pan F, Ye T, Sun P, Gui S, Liang B, Li L, et al. Time course of lung changes at chest CT during recovery from coronavirus disease 2019 (COVID-19). Radiology 2020 Feb;295(3):715–21. https://doi.org/10.1148/radiol.2020200370.
[9] Wang Y, Dong C, Hu Y, Li C, Ren Q, Zhang X, et al. Temporal changes of CT findings in 90 patients with COVID-19 pneumonia: a longitudinal study. Radiology 2020 Mar;296(2):E55–64. https://doi.org/10.1148/radiol.2020200843.
[10] Ooi MWX, Rajai A, Patel R, Gerova N, Godhamgaonkar V, Liong SY. Pulmonary thromboembolic disease in COVID-19 patients on CT pulmonary angiography – prevalence, pattern of disease and relationship to D-dimer. Eur J Radiol 2020 Nov;132:109336. https://doi.org/10.1016/j.ejrad.2020.109336.
[11] Fois AG, Paliogiannis P, Scano V, Cau S, Babudieri S, Perra R, et al. The systemic inflammation index on admission predicts in-hospital mortality in COVID-19 patients. Molecules 2020 Nov;25(23):5725. https://doi.org/10.3390/molecules25235725.
[12] Mitchell C, Rahko PS, Blauwet LA, Canaday B, Finstuen JA, Foster MC, et al. Guidelines for performing a comprehensive transthoracic echocardiographic examination in adults: recommendations from the American Society of Echocardiography. J Am Soc Echocardiogr 2019 Sep;32(1):1–64. https://doi.org/10.1016/j.echo.2018.06.004.

[13] Tei C, Nishimura RA, Seward JB, Tajik AJ. Noninvasive Doppler-derived myocardial performance index: correlation with simultaneous measurements of cardiac catheterization measurements. J Am Soc Echocardiogr 1997 Mar;10(2):169–78. https://doi.org/10.1016/S0894-7317(97)70090-7.
[14] Ghio S, Recusani F, Klersy C, Sebastiani R, Laudisa ML, Campana C, et al. Prognostic usefulness of the tricuspid annular plane systolic excursion in patients with congestive heart failure secondary to idiopathic or ischemic dilated cardiomyopathy. Am J Cardiol 2000 2000/04/01/;85(7):837–42. https://doi.org/10.1016/S0002-9149(99)00877-2.
[15] DiLorenzo MP, Bhatt SM, Mercer-Rosa L. How best to assess right ventricular function by echocardiography. Cardiol Young 2015 Dec;25(8):1473. http://doi:10.1017/S1047951115002255.
[16] Melužín J, Špinarová L, Bakala J, Toman J, Krejčí J, Hude P, et al. Pulsed Doppler tissue imaging of the velocity of tricuspid annular systolic motion. A new, rapid, and non-invasive method of evaluating right ventricular systolic function. Eur Heart J 2001 Feb;22(4):340–8. https://doi.org/10.1053/euhj.2000.2296.
[17] Szekely Y, Lichter Y, Taieb P, Banai A, Hochstadt A, Merdler I, et al. Spectrum of cardiac manifestations in COVID-19: a systematic echocardiographic study. Circulation 2020 Jul;142(4):342–53. https://doi.org/10.1161/CIRCULATIONAHA.120.047971.
[18] Pang L, Stahl EP, Fujikura K, Chen M, Li W, Zhang M, et al. Echocardiography abnormal findings and laboratory operations during the COVID-19 pandemic at a high volume center in New York City. Healthcare 2020 Dec;8(4):534. https://doi.org/10.3390/healthcare8040534.
[19] Lippi G, Lavie CJ, Sanchis-Gomar F. Cardiac troponin I in patients with coronavirus disease 2019 (COVID-19): evidence from a meta-analysis. Prog Cardiovasc Dis 2020 May-Jun;63(3):390–1. https://doi.org/10.1016/j.pcad.2020.03.001.
[20] Yao XHLT, He ZC, Ping YF, Liu HW, Yu SC, et al. A pathological report of three COVID-19 cases by minimal invasive autopsies. Chin J Pathol 2020 May;49(5):411–7. https://doi.org/10.3760/cma.j.cn112151-20200312-00193.
[21] Tavazzi G, Pellegrini C, Maurelli M, Belliato M, Sciutti F, Bottazzi A, et al. Myocardial localization of coronavirus in COVID-19 cardiogenic shock. Eur J Heart Fail 2020 Apr;22(5):911–5. https://doi.org/10.1002/ejhf.1828.
[22] Mansueto G. COVID-19: brief check through the pathologist's eye (autopsy archive). Pathol Res Pract 2020 Nov;216(11):153195. https://doi.org/10.1016/j.prp.2020.153195.
[23] Varga Z, Flammer AJ, Steiger P, Haberecker M, Andermatt R, Zinkernagel AS, et al. Endothelial cell infection and endotheliitis in COVID-19. Lancet 2020 Apr;395(10234):1417–8. https://doi.org/10.1016/S0140-6736(20)30937-5.
[24] Agricola E, Beneduce A, Esposito A, Ingallina G, Palumbo D, Palmisano A, et al. Heart and lung multimodality imaging in COVID-19. JACC (J Am Coll Cardiol): Cardiovasc. Imag. 2020 Aug;13(8):1792–808. https://doi.org/10.1016/j.jcmg.2020.05.017.
[25] Li Y, Li H, Zhu S, Xie Y, Wang B, He L, et al. Prognostic value of right ventricular longitudinal strain in patients with COVID-19. Cardiovasc. Imag. 2020 Nov;13(11):2287–99. https://doi.org/10.1016/j.jcmg.2020.04.014.
[26] Citro R, Pontone G, Bellino M, Silverio A, Iuliano G, Baggiano A, et al. Role of multimodality imaging in evaluation of cardiovascular involvement in COVID-19. Trends Cardiovasc Med 2021 Jan;31(1):8–16. https://doi.org/10.1016/j.tcm.2020.10.001.
[27] Barman HA, Atici A, Tekin EA, Baycan OF, Alici G, Meric BK, et al. Echocardiographic features of patients with COVID-19 infection: a cross-sectional study. Int J Cardiovasc Imag 2021 Mar;37(3):825–34. https://doi.org/10.1007/s10554-020-02051-9.
[28] Szekely Y, Lichter Y, Hochstadt A, Taieb P, Banai A, Sapir O, et al. The predictive role of combined cardiac and lung ultrasound in coronavirus disease 2019. J Am Soc Echocardiogr 2021 Jun;34(6):642–52. https://doi.org/10.1016/j.echo.2021.02.003.
[29] Felsenstein S, Herbert JA, McNamara PS, Hedrich CM. COVID-19: immunology and treatment options. Clin Immunol 2020 Jun;215:108448. https://doi.org/10.1016/j.clim.2020.108448.
[30] Giamarellos-Bourboulis EJ, Netea MG, Rovina N, Akinosoglou K, Antoniadou A, Antonakos N, et al. Complex immune dysregulation in COVID-19 patients with severe respiratory failure. Cell Host Microbe 2020 Jun 10;27(6):992–1000. https://doi.org/10.1016/j.chom.2020.04.009. e1003.
[31] Qin C, Zhou L, Hu Z, Zhang S, Yang S, Tao Y, et al. Dysregulation of immune response in patients with coronavirus 2019 (COVID-19) in Wuhan, China. Clin Infect Dis 2020 Jul 28;71(15):762–8. https://doi.org/10.1093/cid/ciaa248.
[32] Chung M, Bernheim A, Mei X, Zhang N, Huang M, Zeng X, et al. CT imaging features of 2019 novel coronavirus (2019-nCoV). Radiology 2020 Apr;295(1):202–7. https://doi.org/10.1148/radiol.2020200230.
[33] Bernheim A, Mei X, Huang M, Yang Y, Fayad ZA, Zhang N, et al. Chest CT findings in coronavirus disease-19 (COVID-19): relationship to duration of infection. Radiology 2020 Jun;295(3):200463. https://doi.org/10.1148/radiol.2020200463.
[34] Salehi S, Abedi A, Balakrishnan S, Gholamrezanezhad A. Coronavirus disease 2019 (COVID-19): a systematic review of imaging findings in 919 patients. Am J Roentgenol 2020 2020/07/01;215(1):87–93. https://doi.org/10.2214/AJR.20.23034.
[35] Yang R, Li X, Liu H, Zhen Y, Zhang X, Xiong Q, et al. Chest CT severity score: an imaging tool for assessing severe COVID-19. Radiology: Cardiothorac. Imag. 2020 Mar 30;2(2):e200047. https://doi.org/10.1148/ryct.2020200047.
[36] Huang L, Han R, Ai T, Yu P, Kang H, Tao Q, et al. Serial quantitative chest ct assessment of covid-19: deep-learning approach. Radiology: Cardiothorac. Imag. 2020 Mar 30;2(2):e200075. https://doi.org/10.1148/ryct.2020200075.
[37] Yuan M, Yin W, Tao Z, Tan W, Hu Y. Association of radiologic findings with mortality of patients infected with 2019 novel coronavirus in Wuhan, China. PloS One 2020 Mar 19;15(3):e0230548. https://doi.org/10.1371/journal.pone.0230548.
[38] Baycan OF, Barman HA, Atici A, Tatlisu A, Bolen F, Ergen P, et al. Evaluation of biventricular function in patients with COVID-19 using speckle tracking echocardiography. Int J Cardiovasc Imag 2021 Jan;37(1):135–44. https://doi.org/10.1007/s10554-020-01968-5.